International Journal of Electrical and Electronics Engineering (IJEEE)
ISSN(P): 2278-9944; ISSN(E): 2278-9952
Vol. 6, Issue 1, Dec - Jan 2017, 15-26

International Academy of Science, Engineering and Technology
Connecting Researchers; Nurturing Innovations

DETECTION AND LOCALIZATION OF A MOVING PERSON BEHIND THE WALL BASED ON BILATERATION TECHNIQUE

BETÜL YILMAZ[1], CANER ÖZDEMIR[2] & ALI AKDAĞLI[3]

[1,2,3]Department of Electrical and Electronics Engineering, Mersin University,
Ciftlikkoy, Mersin, Turkey

[2] Emtech IT Technologies Engineering Corp, Mersin Technology Development Zone,
Yenişehir, Mersin, Turkey

ABSTRACT

In this paper, we present an effective technique to detect and localize a moving target behind the wall. The method based on one transmitter and two receiver antenna system configuration. The precision of the method is first surveyed by simulating a hypothetical target. Then, the algorithm is tested with a real data gathered from a measurement that was accomplished behind a brick wall with an ultra-wide-band (UWB) transceiver system. Thru-the-wall radar imaging results show that algorithm successfully detects and indicates the correct locations of a moving person behind the wall. Our numerical and experimental studies in this work clearly demonstrate that the proposed method can be appropriately used in similar TWR applications or localization problems.

KEYWORDS: Remote Sensing, Through-The-Wall Radar, Moving Target Detection, Radar Signal Processing, Localization Algorithm

1. INTRODUCTION

Through-wall radar (TWR) is has been an highly developing technology for detecting and localizing persons/objects behind the wall or any opaque obstacle [1-3]. TWR has many practices ranging from civil applications such as earthquake/fire rescue operations to military ones including detecting terrorists inside buildings [1-5]. For the TWR design, ultra-wide band (UWB) time-domain radar systems are thought to be more advantageous to frequency domain counterparts since they can operate faster and also maintain high resolution features with much higher signal power levels for better penetration and deeper detection ranges [5-6]. For these advantageous properties, many scientists have utilized UWB time-domain TWR usage by applying various detection/localization techniques to focus and image objects or human movement behind walls [6-10]. One of the promising methods is called the back-projection algorithm (BPA) which has been also applied successfully in conventional synthetic aperture radar (SAR) applications [11-14]. Although BPA has been frequently used in TWR imaging usages, its summation step causes undesired artifacts in the form of long side lobes that negatively affect the resolutions in the constructed images. Similar to BPA, other focusing techniques such as Kirchoff Migration [15] and f-k migration [16] have the main disadvantage of being slow due to iterative summation step within the algorithm. In addition to these well-known robust focusing methods, some high-resolution techniques have also been applied by some researchers in pursuit of having better detection outcomes [17-19]. One of the most promising candidate is the beams pace multiple signal classification algorithm (BS-MUSIC) that have the ability to provide highly resolved images [17]. On the other hand, it requires the a priori knowledge of some parameters of scene such as wall thickness and

the wall's dielectric constant. Furthermore, MUSIC is quite slow while computing the estimate of the covariance matrix and array response vector. Sparse Tomographic Inverse Scattering Approach [18] and an autofocusing technique, based on higher order statisticsmethod [19] have also been applied for seeking a good performance on detection with a fine resolution metrics. They require coherent processing of the collected data sets that cannot be practical in most TWR applications.

In this work, we have presented a non-coherent technique based on geometrical bilateration approach for one-transmitter two-receiver TWR set-up. This method mainly calculates the intersection point of the two ellipses that are formed by one-transmitter one-receiver pairs. This paper is organized as follows: In the next section, the imaging algorithm based on intersection of ellipses is described with details. In Section 3, the simulation results are presented to assess the performance of the algorithm. In Section 4, the algorithm is tested by the real data collected with a UWB time domain radar system to detect and locate a moving human behind a brick wall. In the last section, the discussion about the cons and pros of the implemented algorithm are given and the work is concluded.

2. LOCALIZATION ALGORITHMBASED ON BILATERATION TECHNIQUE

Our detection and localization algorithm relies on the assumptions that the wall thickness is small compared to target range and the dielectric permittivity of the wall medium (ϵ_r) is not high. In fact, these assumptions generally hold true provided that the practical wall thickness generally ranges from 15 cm to 40 cm and ϵ_r varies from 1.5 to 6 for wooden, brick and/or concrete walls [20]. With this construct, the amount of shift between the actual location and the estimated location of the target (d_{shift}) is negligible as illustrated in Figure 1. The error associated with this assumption has been studied in detail in [21].

The principle of our algorithm is based on multi-static geometry in which a transmitting antenna (*Tx*) and two receiving antennas ($Rx_1$and Rx_2)are positioned behind the wall as illustrated in Figure 1. As shown from the figure, as the *Tx* is situated in the middle and $Rx_1$and Rx_2 are put at the same distance of D away from *Tx* along the cross-range axis (x). The distance from *Tx* to point target; r_0 and the distances from point target to$Rx_i (i = 1, 2)$; r_1 andr_2, are estimated by the help of round trip time and the speed of the electromagnetic (EM) wave. In fact; the locations of *Tx*and Rx_i scorrespond to the focal points of the ellipse curves. Therefore; the sum of the distances from the foci to any points on the ellipses $(r_0 + r_1, r_0 + r_2)$ are constant and they are equal to the horizontal major axis of $2a$. For our radar geometry; two elliptic curves are occurred due to two receivers. The equations of these two ellipses centered at $(-D/2,0)$ and $(D/2,0)$ with respect to the x and y-axis as;

$$\frac{(x+D/2)^2}{{a_1}^2} + \frac{y^2}{b^2} = 1 \quad (1)$$

$$\frac{(x-D/2)^2}{{a_2}^2} + \frac{y^2}{b^2} = 1 \quad (2)$$

Here; semi-major axes ($a_1$and a_2); and semi-minor axes (b_1 and b_2) of two ellipses according to Figure 1 are described as below:

$$\begin{aligned} a_1 &= r_0 + r_1 \\ a_2 &= r_0 + r_2 \end{aligned} \quad (3)$$

$$b_1 = \sqrt{{a_1}^2 - (D/2)^2}$$
$$b_2 = \sqrt{{a_2}^2 - (D/2)^2} \quad (4)$$

It is assumed that there is a perfect point scatter as a target behind the wall as shown in Figure. 1 and its location $P(x_0, y_0)$ can be simply obtained by intersection of these two ellipses which are defined in Eqn. (1) and Eqn. (2), respectively. The formulation steps in calculating the intersection of these curves are expressed briefly as follows;

$$A = {a_2}^2 \cdot {b_1}^2 - {a_1}^2 \cdot {b_2}^2$$
$$B = D \cdot \left({a_2}^2 \cdot {b_1}^2 + {a_1}^2 \cdot {b_2}^2\right) \quad (5)$$
$$C = (D/2)^2 \cdot A + {a_1}^2 \cdot {a_2}^2\left({b_2}^2 - {b_1}^2\right)$$

$$x_{1,2} = -\frac{B \mp \sqrt{B^2 - 4AC}}{2A}$$
$$y = \sqrt{{b_2}^2 \cdot \left(1 - \frac{\left(x_{1,2} - D/2\right)^2}{{a_2}^2}\right)} \quad (6)$$

Where A, B and C are the coefficients of the quadratic polynomial of $Ax^2 + Bx + C = 0$. Then, the cross-range location (x) and the range position (y) of the point target behind the wall can be calculated by finding the roots of this polynomial and solving Eqn. (6). In fact, this equation set yields two dual solutions of (x_1, y_1) and (x_2, y_2). Based on the assumed geometry in Figure 1; of course, the positive notation for the range value (y) should be chosen as the solution that will give only one set of either (x_1, y_1) or (x_2, y_2).

SIMULATION SCENARIO

We have constructed a simulation scenario in Matlab programming [22] to assess the performance of the proposed detection and localization algorithm. For this goal, a hypothetical moving target was considered. In the simulation, we have chosen the separation of antennas at $D = 30\ cm$ as seen in Figure 2 where the geometry of the scenario is given. The frequency of the radar system was altered from 1 GHz to 6GHz for a total of 200 discrete frequencies in stepped-frequency radar configuration. Firstly, the starting point of moving target was assumed at point $P(1,3)$ on the range (y) and cross-range (x) plane. Then, it was reached up to point $P'^{(-1,3)}$ by a curved path for a total of 18 distinct target locations as shown in Figure 2. So, the frequency diverse two-dimensional (2D) scattered electric field data; $E_1^S(k,\tau)$ and $E_2^S(k,\tau)$ were collected by the receivers at different time instants of τ_i as

$$E_1^S(k,\tau_i) = \sigma_1 \cdot e^{-jk(r_{0i} + r_{1i})}$$
$$E_2^S(k,\tau_i) = \sigma_2 \cdot e^{-jk(r_{0i} + r_{2i})} \quad i = 1,2,\ldots 18 \quad (10)$$

Here; σ_1 and σ_2 are the EM reflectivity constants for the first and the second receiver, respectively. For this simulation, they were assumed to be independent from frequency and aspect angle so that $\sigma_1 = \sigma_2 = 1$. Now, we can get the bi-static ranges of these collected scattered electric field data by taking the one dimensional (1D) inverse Fourier transform (IFT) of $E_1^S(k,\tau)$ and $E_2^S(k,\tau)$ with respect to wave-number; k. Then, the 2D range-time scattered field vector sets of $E_1^S(r,\tau)$ and $E_2^S(r,\tau)$ were obtained as plotted in Figure 3 (a) and Figure 3 (b), respectively. As shown from these range profiles, the movement of point scatterer can be easily observed. Next, the terms of semi-major axes $(a_1$ and $a_2)$ and semi-minor axes $(b_1$ and $b_2)$ were calculated that were explained in the previous section. Then, the steps of the algorithm were employed in the above-mentioned successive order to obtain the range (y) and cross-range (x) coordinates of 18

different scene snapshots. In Figure 4, employment of the bilateration technique has been realized for three different time instants. The ellipse that corresponds to the first receiver was drawn as red dashed line whereas the one that corresponds to the second receiver was drawn as blue dashed line. The intersections of the ellipses are represented as black dots. In Figure 5, both the real locations (drawn as black circles) and the estimated locations (plotted as magenta crosses) by our algorithm of the moving target for different 18 time instants are plotted. The visual comparison of these two results clearly demonstrates how our algorithm successfully detects and pinpoints the locations of the moving point-scatterer with a reliable prediction.

MEASUREMENT RESULTS

After validating the accuracy of the algorithm by the help of synthetic scenario, the algorithm was tested with a real data collected by an experimental test-bed. For this goal, an experimental scenario whose geometry as shown in Figure 6 was formed. *Tx* antenna was placed at (0, 0) and two *Rx* antennas were positioned equally spaced as $30\ cm$ on either side of it. Additionally; the antenna configuration was positioned $5\ cm$ away against a $20\ cm$ thick brick wall. During the experiment, a male human was stood behind the wall and walked away and towards the wall twice during the time period of $21\ s$. As it can be observed clearly from the Figure 6; the man started to walk at a radial distance of $0.35\ m$ from the *Tx* antenna and returned from$4.1\ m$ in the first-round trip. In his second-round walk; he followed the same route and trip was ended at $2.4\ m$ radial distance from the transmitter.

Our experimental measurement system is shown in Figure 7. The measurement set-up was composed of an Analog/Digital convertor (Geozondas GZ6E) and pulse generator head (GZ1118GN-01EV) which was used as the time domain transceiver system as seen Figure 7 (a). Also, we used one *Tx* and two *Rx* horn antennas that can work between 1 and 6 GHz. For the automatic control of the whole system, we have developed a Matlab script. While the man was walking behind the wall (see Figure 7 (b)), we collected consecutive92time domain responses of the scene during the $21\ s$ period. The collected raw data from Rx_1 and Rx_2 are as depicted in Figure 8 (a) and (b), respectively. We can see from the figures that signals which were shown at $r = 0$ represented the cross-talk between *Tx* and the *Rx* antennas and also taken as the phase center of our experiment. The wall was seen from $r = 0.15\ m$ to $r = 0.35\ m$ as the highest echo shown up as the straight lines in all 1D range profiles. Then, we have applied the background subtraction procedure to raw dataset to improve the signal-to-noise ratio(SNR) and also to remove the artifacts caused by the wall. Sequential differentiation process has been applied by subtracting the images in a sequential order. Thus, the stationary objects and other undesirable clutters were suppressed and the reflections of man's walking were substantially raised up as shown in Figure 9 (a) and (b) for the first and the second receiver, respectively. When $t = 5.8\ s$, the man was about $3.75\ m$ away from the wall and it took $6.1\ s$ to reach the nearest position and he returned the same range location as shown in Figure 9. Weapplied the steps of our implementation for the bilateration technique that was described in Section 2. Figure 10 shows the red and blue elliptic curves that were collected by Rx_1 and Rx_2, respectively. The black dots on these curves indicate the intersection point of these two ellipses calculated with the proposed method at different time instants. In Figure 11, the estimated locations of the person between $\mathrm{t} = 5.8$ s and $\mathrm{t} = 17.1$ s are plotted. These results are in very good agreement with the real positions of the walking target during his round-trip movement.

CONCLUSIONS

In this paper, we have proposed and implemented a method based on the range profile knowledge from the

receiving antennas that was positioned at both side of the transmitting antenna for TWR usage to detect and localize a target behind an opaque obstacle. The algorithm relies on the estimation of intersecting the ellipses formed by 1-Tx and 1-Rx pair for the two receivers. The proposed method was examined with both a simulation data constructed in Matlab environment and the real data from a UWB time-domain radar system. The resultant detection and localization performance of the algorithm clearly demonstrate the validity and the success of the proposed approach.

This algorithm has the advantage of being very fast since the location of the target is directly calculated by taking 1D range profile measurement and applying the analytical formula given in Eqns. (5) and (6). Therefore, real-time detection and localization of the target is realized. On the other hand, this approach has the disadvantage of detecting only one movement since the intersection line of more than two ellipses will produce many intersections. While some of these intersections (i.e., 1-1, 2-2, 3-3,.. etc.) would represent the exact locations of the target, other intersecting locations (i.e., 1-2, 2-1, 1-3, 3-1 2-3, 3-2,.. etc.). would produce hypothetical, ghost targets. As the future research; therefore, this algorithm can be further improved to detect and locate multiple targets behind the wall by taking care of this ghost crossing problem.

ACKNOWLEDGEMENTS

This work is supported by the Scientific and Research Council of Turkey (TUBITAK) under grant no: TEYDEB-7151335 and by Mersin University Scientific Research Unit under Project No. BAP-FBE EEM (BY) 20117DR. The authors are thankful to Mustafa Berkan Biçer and Volkan Yamaçlı for their help during the experiment.

REFERENCES

1. D.D. Ferris, Jr. and N.C. Currie, A survey of current technologies for through-the-wall surveillance, *Proc. SPIE* **3577**, (1998), 62-72.
2. E.J. Baranoski, Through-wall imaging: Historical perspective and future directions, *J. Franklin Inst.***345**, (2008), 556-569.
3. J.E. Peabody, G.L. Charvat, J. Goodwin, and M. Tobias, Through-wall imaging radar,*Lincoln Lab. J.*, **19**, (2012), 62–72.
4. H.D. Griffiths and C.J. Baker, Radar imaging for combatting terrorism, Imaging for Detection and Identification NATO Security through Science Series Springer, Netherlands, 2007, 29-48.

a. Martone, K. Ranney, and R. Innocenti, Automatic through the wall detection of moving targets using low-frequency ultra-wideband radar,*2010 IEEE Radar Conference*, (2010), 39–43.

5. R. S. Thoma, O. Hirsch, J. Sachs and R. Zetik,UWB Sensor Networks for Position Location and Imaging of Objects and Environments, *The Second European Conference on Antennas and Propagation EuCAP 2007*, (2007), 1-9.
6. J. Rovňáková and D. Kocur, TOA Estimation and Data Association for Through-Wall Tracking of Moving Targets, *EURASIP Journal on Wireless Communications and Networking 2010*, (2010), 11 pages.
7. D. Yipeng, S. Kehui and X. Xuemei, Hough-MHAF localization algorithm for dual-frequency continuous-wave through-wall radar,*IEEE Transactions on Aerospace and Electronic Systems* **52**, (2016), 111-121.

8. S. Wu and G. Fang, Detection and Tracking of Moving Target behind Wall Using UWB Through-wall Radar, *2010 International Conference on Intelligent System Design and Engineering Application*, (2010), 605-608.

9. H. Wang, R.M. Narayanan and Z.O. Zhou, Through-Wall Imaging of Moving Targets Using UWB Random Noise Radar, *IEEE Antennas and Wireless Propagation Letters* **8**, (2009), 802-805.

10. F. Ahmad, M. G. Amin and S. A. Kassam, Synthetic aperture beamformer for imaging through a dielectric wall, *IEEE Transactions on Aerospace and Electronic Systems* **41**, (2005), 271-283.

a. Franchois, P. Lewyllie, L. Taerwe, 2-D near-field SAR non-destructive testing of rebars in a concrete wall, *International Journal of Applied Electromagnetics and Mechanics* **19**, (2004), 333-338

11. Ş. Demirci, E. Yiğit, İ. H. Eskidemir, C. Özdemir, Ground penetrating radar imaging of water leaks from buried pipes based on back-projection method, *Independent Nondestructive Testing and Evaluation* **47**, (2012), 35-42.

12. C. Özdemir, Inverse Synthetic Aperture Radar Imaging with MATLAB Algorithms, John Wiley & Sons, 2012, ISBN: 978-0-470-28484-1.

13. S. Wu, K. Tan, Y. Xu, J. Chen, S. Meng and G. Fang, A simple strategy for moving target imaging via an experimental UWB through-wall radar,*14th International Conference on Ground Penetrating Radar (GPR)*, (2012), 961-965.

14. T. Sakamoto, T. Sato, P. J. Aubry and A. G. Yarovoy, Ultra-Wideband Radar Imaging Using a Hybrid of Kirchhoff Migration and Stolt F-K Migration With an Inverse Boundary Scattering Transform,*IEEE Transactions on Antennas and Propagation* **63**, (2015), 3502-3512.

15. Y.S. Yoon and M.G. Amin, High-Resolution Through-the-Wall Radar Imaging Using Beamspace MUSIC, *IEEE Transactions on Antennas and Propagation* **56**, (2008) 1763-1774.

16. F. Soldovieri, R. Solimene and F. Ahmad, Sparse Tomographic Inverse Scattering Approach for Through-the-Wall Radar Imaging, *IEEE Transactions on Instrumentation and Measurement* **61**, (2012), 3340-3350.

17. F. Ahmad, M. G. Amin and G. Mandapati, Autofocusing of Through-the-Wall Radar Imagery Under Unknown Wall Characteristics, *IEEE Transactions on Image Processing* **16**, (2007), 1785-1795.

18. C. Thajudeen, A. Hoorfar, F. Ahmad and T. Dogaru, Measured complex permittivity of walls with different hydration levels and the effect on power estimation of TWRI target returns, *Progress In Electromagnetics Research B* **30**, (2011), 177-199.

19. P.H. Chen, R.M. Narayanan, Shifted Pixel Method for Through-Wall Radar Imaging, *IEEE Transactions on Antennas and Propagation* **60**, (2012), 3706-3716.

20. http: //www.mathworks.com/products/matlab/[Accessed 12December 2016]

FIGURE CAPTIONS

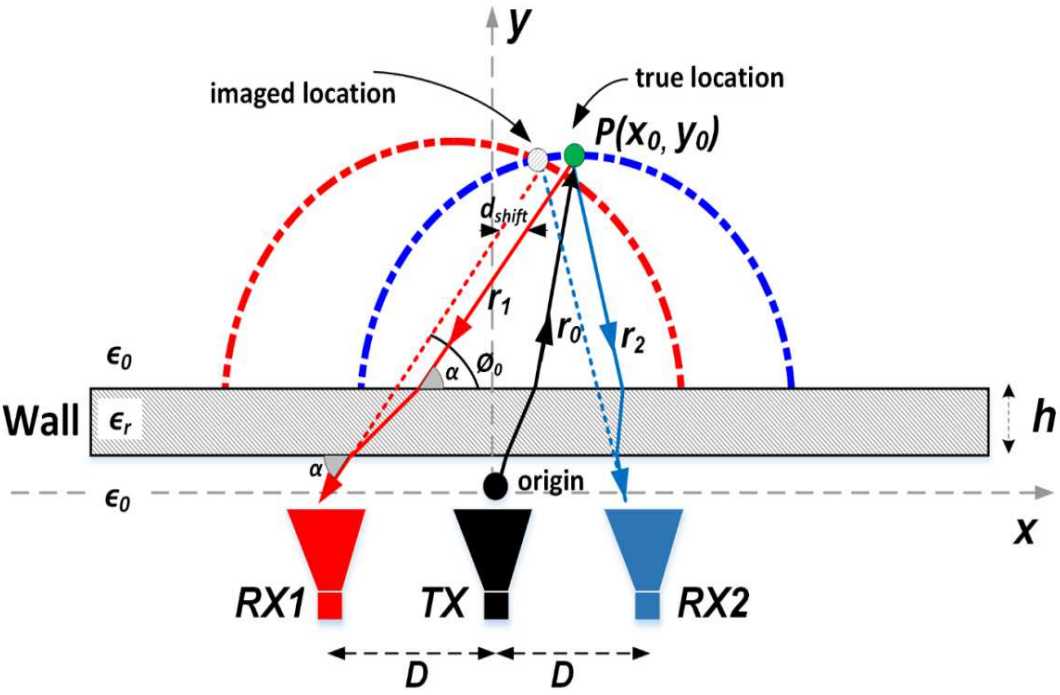

Figure 1: Through-The-Wall Radar Geometry of Bilateration Method

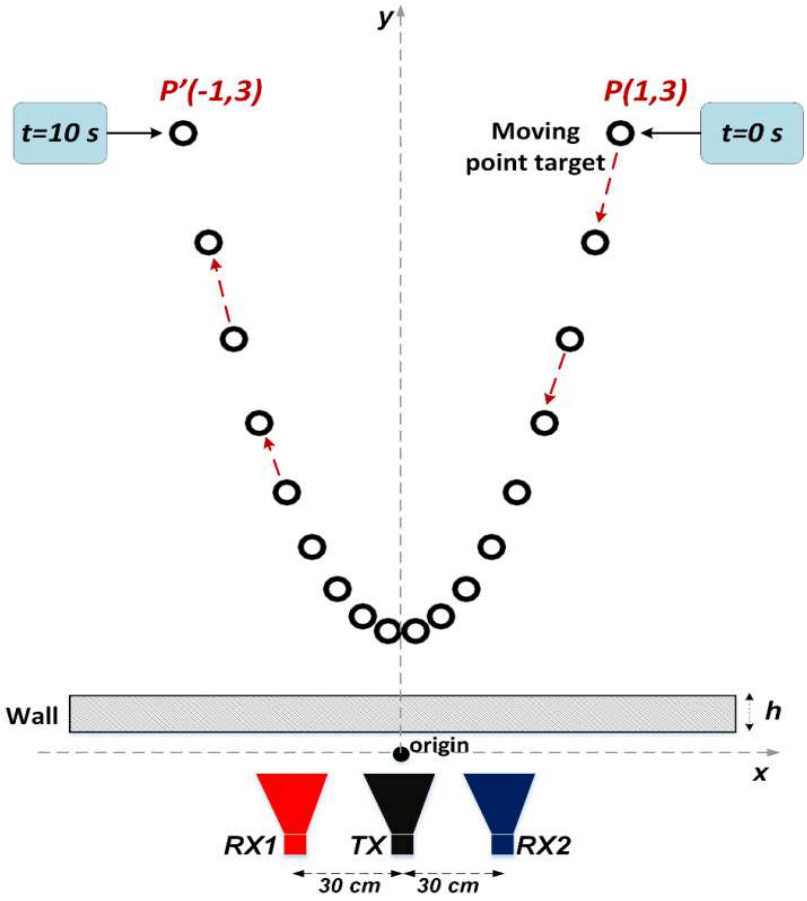

Figure 2: Geometry of Simulation Scenario

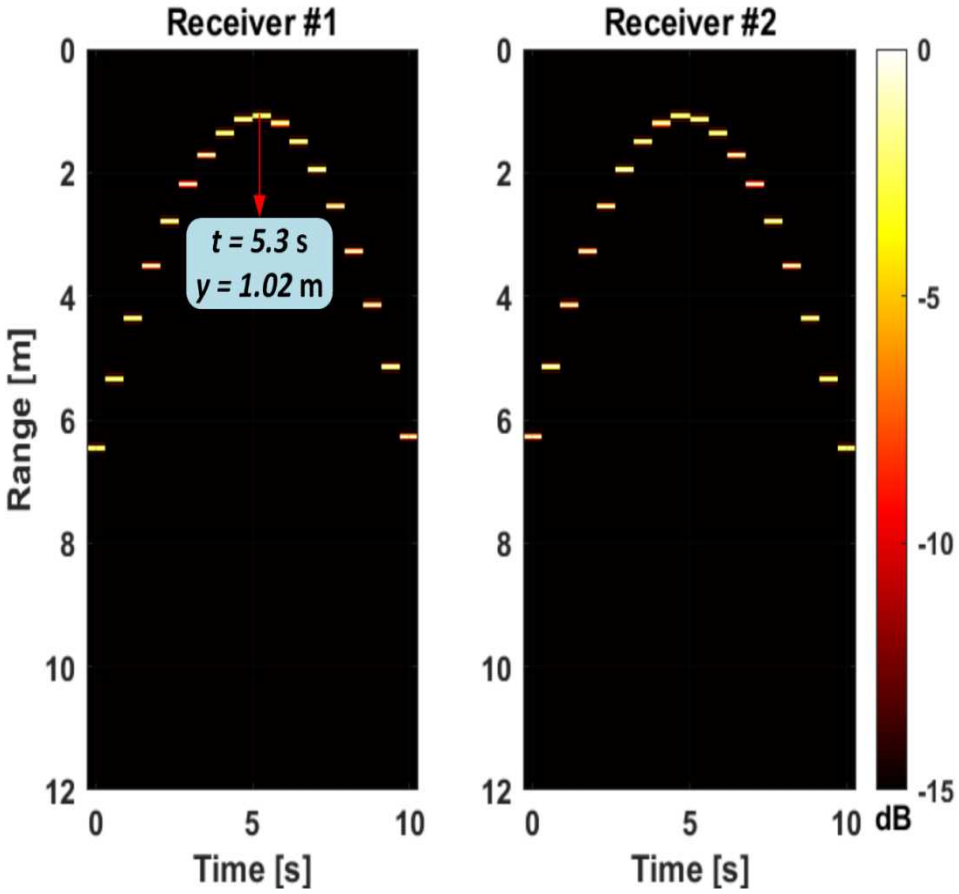

Figure 3: Bistatic Range Profiles for (A) Receiver #1 and (B) Receiver #2 for Different Time Instants from t_1To t_{18}

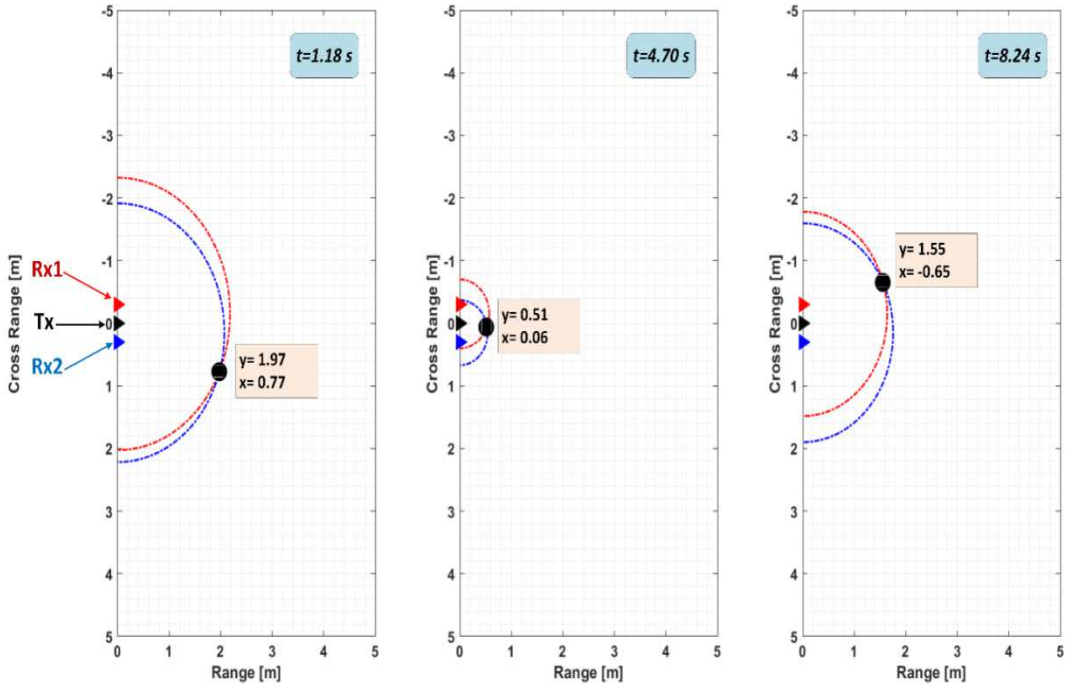

Figure 4: Elliptic Curves Related to Receiver #1 [Drawn As Red] and Receiver #2 [Drawn As Blue] and Intersection Points of These Curves for Three Different Time Instants for Simulation Results

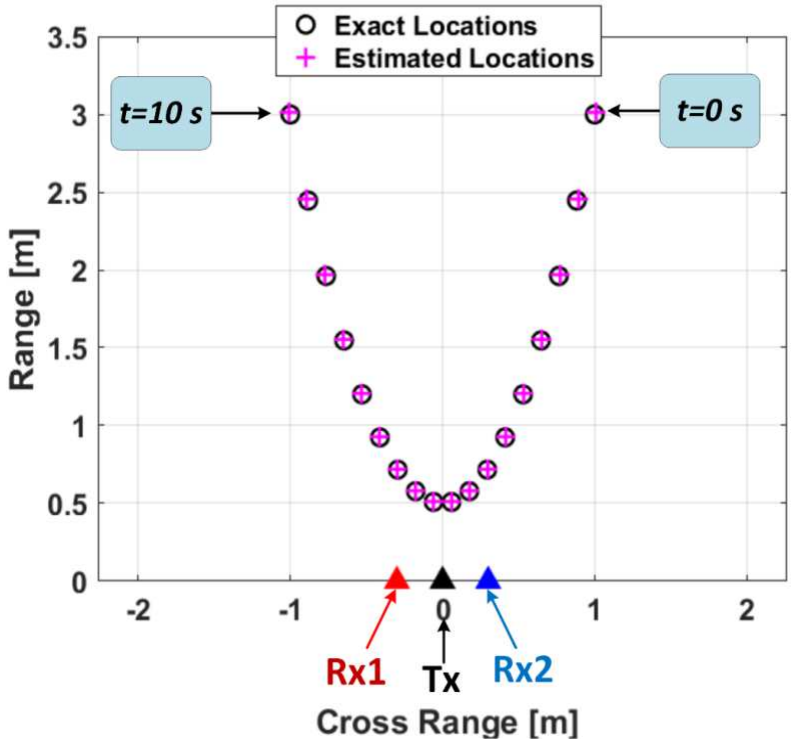

Figure 5: True Locations (Black Circles) and Estimated Locations (Magenta Crosses) of Human Target Locations after the Algorithm

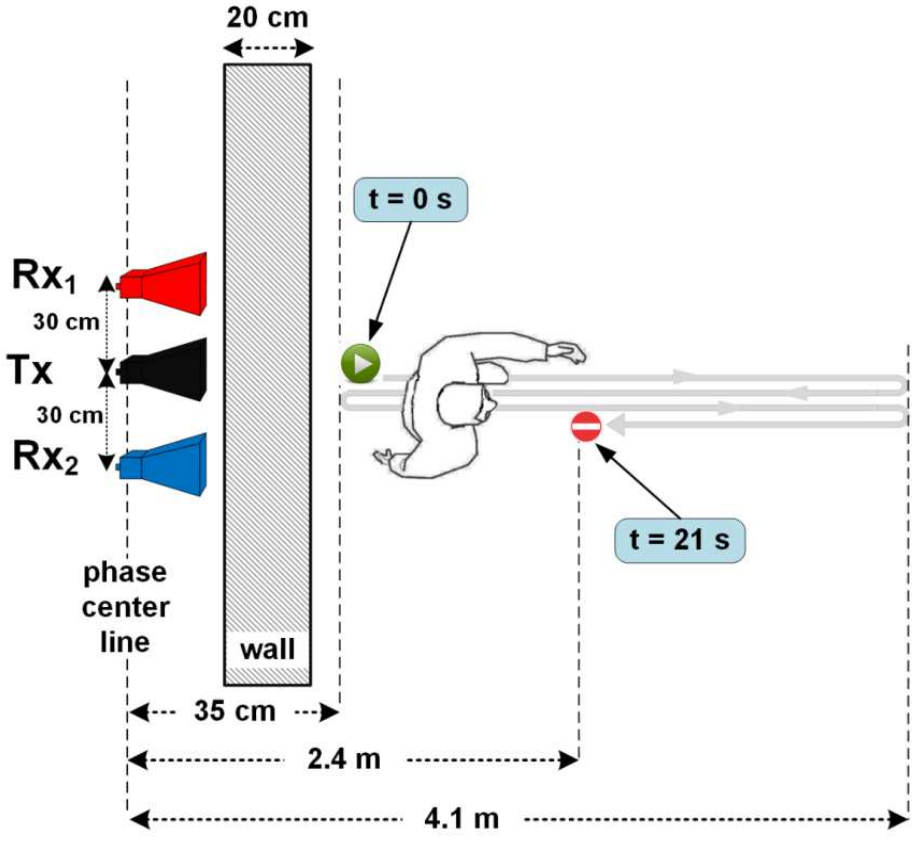

Figure 6: The Geometry of the Measurement Geometry: Human Walking Towards and Away from the Wall

(a)

(b)

Figure 7: (a) A Picture of the Experimental Set-Up, (b) A Scene From the Measurement: Human Walking Away and Towards the Wall

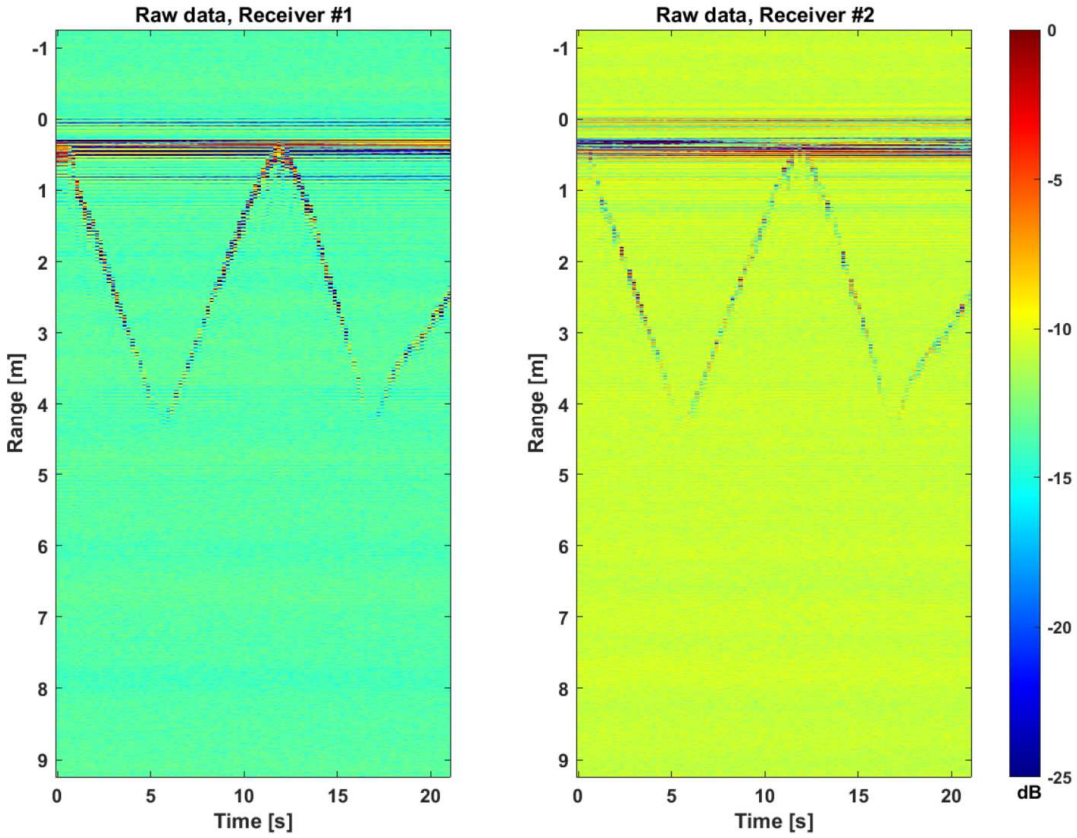

Figure 8: The Raw Range-Time Images of the Collected Data Sets

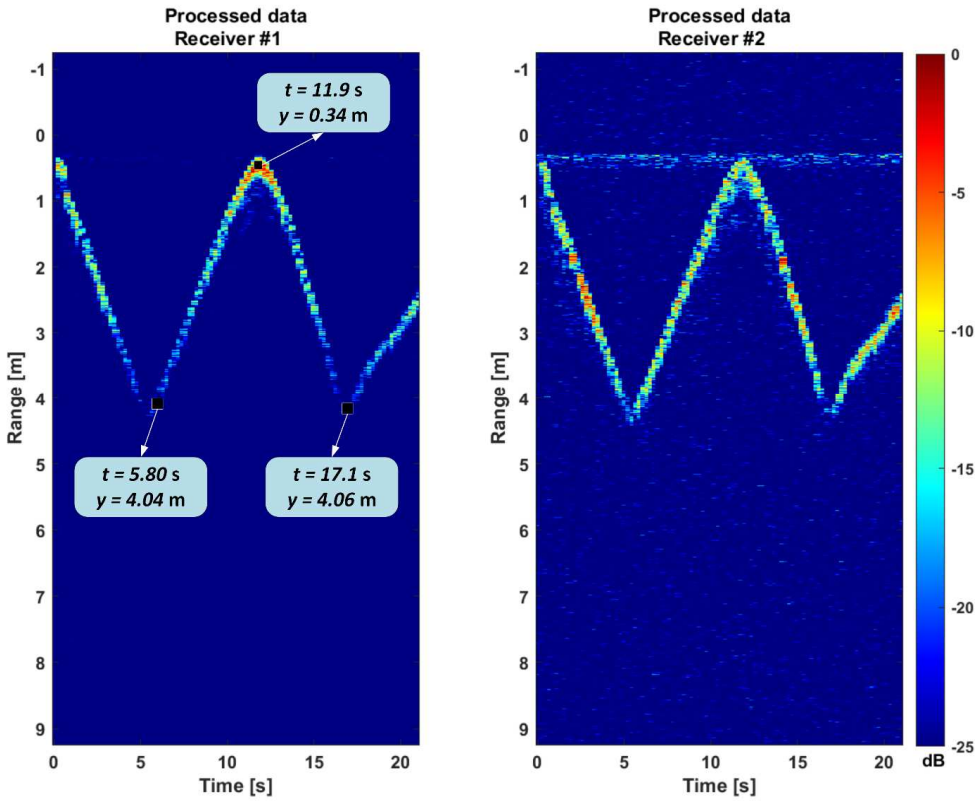

Figure 9: The Differentiated Range-Time Images of the Collected Data Sets

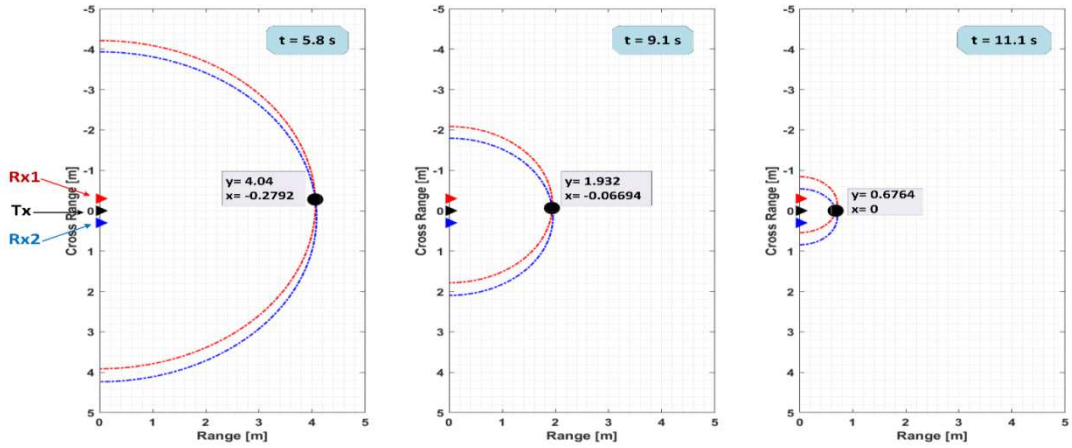

Figure 10: Measured Elliptic Curves Related to Receiver #1[Drawn as Red] and Receiver #2 [Drawn as Blue] and Intersection Points of Thesecurves for Three Different Time Instants

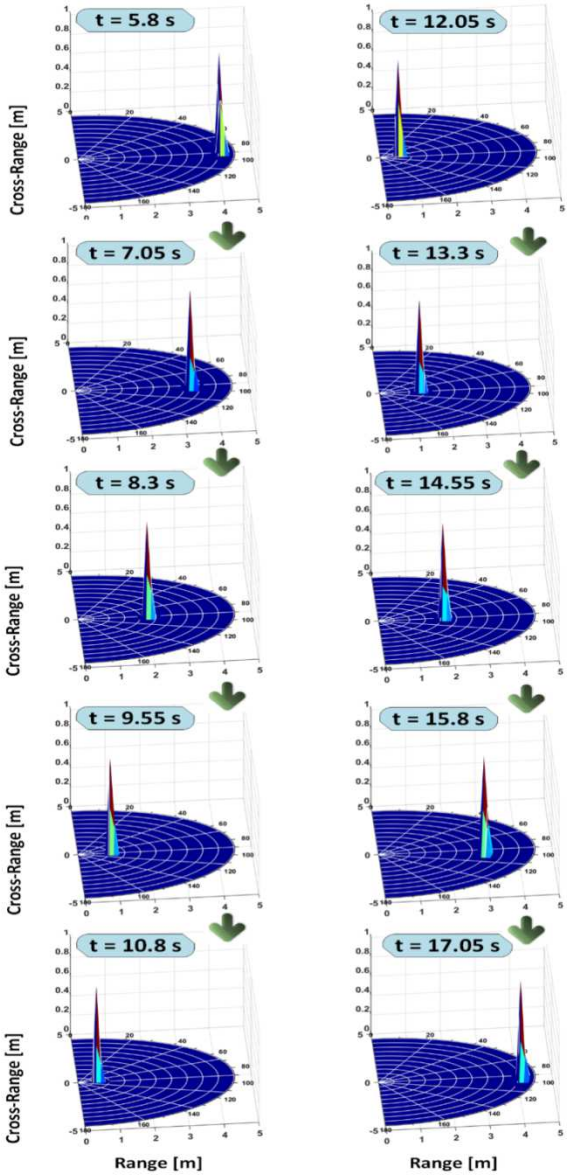

Figure 11: Calculated Locations of the Walking Man after Applying the Algorithm